



Research article

Carbon dioxide dynamics in a residential lawn of a tropical city

Erik Velasco^{a,*}, Elvagrís Segovia^b, Amy M.F. Choong^c, Benjamin K.Y. Lim^c, Rodrigo Vargas^d^a Centre for Urban Greenery and Ecology, National Parks Board, Singapore^b Department of Geography, National University of Singapore, Singapore^c Department of Biological Sciences, National University of Singapore, Singapore^d Department of Plant and Soil Sciences, University of Delaware, Newark, DE, USA

ARTICLE INFO

Keywords:

Turfgrass
 Urban lawn
 Carbon accumulation
 Soil respiration
 Urban carbon sequestration
 Greenery management

ABSTRACT

Turfgrass is an important component of the urban landscape frequently considered as an alternative land cover to offset anthropogenic CO₂ emissions. However, quantitative information of the potential to directly remove CO₂ from the atmosphere by turfgrass systems is lacking, especially in the tropics. Most assessments have considered the carbon accumulated by grass shoots and soil, but not the release of CO₂ to the atmosphere by soil respiration (i.e., soil CO₂ efflux). Here, we measured at high-temporal resolution (30-min) soil CO₂ efflux, production, and storage rate for nearly three years in a residential lawn of Singapore. Furthermore, we quantified the carbon capture related to biomass production and CO₂ emissions from fossil fuel consumption associated with maintenance activities (e.g., mowing equipment). Warm and humid conditions resulted in relatively constant rates of soil CO₂ efflux, CO₂ storage in soil, and aboveground biomass production (3370, 652, 1671 Mg CO₂ km⁻² yr⁻¹; respectively), while the systematic use of mowing machinery emitted 27 Mg CO₂ km⁻² yr⁻¹. Soil CO₂ efflux and CO₂ mowing emissions represent carbon losses to the atmosphere, while CO₂ storage in soil and biomass productivity represent gains of carbon into the ecosystem. Under a steady state in which soil CO₂ losses are only compensated by atmospheric CO₂ uptake by photosynthesis, an ideal clipping waste disposal management, in which no CO₂ molecule returns to the atmosphere (i.e., clippings are not burnt), and a 3-week mowing regime, this site can act as a sink of 2296 Mg CO₂ km⁻² yr⁻¹. In the scenario of incinerating all clippings, the lawn acts as an emission source of 1046 Mg CO₂ km⁻² yr⁻¹. Thus, management practices that reduce mowing frequency together with clipping disposal practices that minimize greenhouse gas emissions are needed to make urban lawns a potential natural solution to mitigate global environmental change.

1. Introduction

Lawns are ubiquitous in urban environments. Plots covered by short-cut grass enhance urban aesthetics and provide open spaces for recreation and sport activities, which is perceived to increase livability and bring about societal benefits (e.g., Vogt et al., 2017). These are strong reasons to promote their expansion without need of citing other potential ecosystem services that have not yet been properly tested. Urban lawns, in general urban vegetation, are purported to reduce water runoff, increase water infiltration, mitigate soil erosion, cool local climate, remove airborne pollutants and offset greenhouse gas emissions, among other positive services (see Monteiro, 2017). Some of these services have been proven, but others are poorly supported by scientific evidence, especially those involving the exchange of mass and energy with the overlaying atmosphere. For example, the capacity of urban

vegetation to improve air quality, mitigate urban heat and offset carbon emissions is still highly uncertain, in contrast to the effectiveness for preventing soil erosion and controlling stormwater runoff (Pataki et al., 2011).

The limited knowledge on urban biogeochemistry and a lack of holistic assessments to evaluate the role of vegetation within the urban ecosystem jeopardize the output of policies promoting greenery to solve environmental problems. For instance, many cities are expanding green areas and planting trees as a mean to curb global environmental change. Studies suggest that parks, gardens, lawns and trees along roadsides may represent important carbon reservoirs and sinks (e.g., Weissert et al., 2014). These studies are usually based on biomass estimates by allometry and growth prediction models, and measurements of carbon changes in underlying soil. They provide valuable insights about the fate of carbon accumulated by urban vegetation, but a) do not directly

* Corresponding author.

E-mail address: velasco@mce2.org (E. Velasco).<https://doi.org/10.1016/j.jenvman.2020.111752>

Received 17 May 2020; Received in revised form 20 November 2020; Accepted 24 November 2020

Available online 24 December 2020

0301-4797/© 2020 Elsevier Ltd. All rights reserved.

quantify the net carbon dioxide (CO₂) removed by photosynthesis from the atmosphere; b) usually neglect the contribution from soil CO₂ efflux (F_s ; CO₂ flux from soil to the atmosphere resulting from autotrophic, i.e., roots and mycorrhizae, and heterotrophic, i.e., microbial activity respiration, sources); and c) do not account for emissions associated with greenery management (e.g., use of machinery for mowing).

Some cities count with bottom-up assessments of the atmospheric carbon sequestered by trees (Nowak et al., 2013), but not of the carbon returned to the atmosphere via F_s . The carbon flux in urban lawns is usually accounted as the sum of carbon removal via clipping harvest and organic matter changes in underlying soil (Guertal, 2012). For example, several studies have measured F_s from urban lawns using soil flux chambers (e.g., Bae and Ryu, 2017; Decina et al., 2016; Weissert et al., 2016; Livesley et al., 2010). A handful of studies has quantified the indirect emissions from mowing, irrigation and fertilization using bottom-up approaches (Zirkle et al., 2011; Townsend-Small and Czimczik, 2010; Jo and McPherson, 1995; Falk, 1976), as well as a few others evaluated the carbon uptake and storage by grass (Jo and McPherson, 1995; Falk, 1980). That said, only one study has evaluated together the CO₂ contributions from F_s , biomass productivity and turf maintenance in urban lawns (Lerman and Contosta, 2019); consequently, integral approaches are needed to close the urban CO₂ budget under managed systems.

Small eddy covariance flux towers provide an alternative approach to evaluate the net atmospheric carbon exchange over turfgrass landscapes including the net contributions from ecosystem respiration and biomass productivity, but their application is challenging due to the typically small dimensions of urban lawns (Pahari et al., 2018; Hiller et al., 2011). An alternative to measure F_s in urban soils is the flux-gradient method, in which the CO₂ exchange is calculated based on the vertical profile of CO₂ concentration and soil gas diffusivity (Maier and Schack-Kirchner, 2014). This method has gained increased attention in the last 15 years, and nowadays is widely applied across natural ecosystems, but not yet in urban lawns or parks according to our knowledge. The flux-gradient method is useful to continuously measure F_s (i.e., in 10–30 min intervals) over years, which allows the detection of short-term variations (e.g., pulses), as well as diel, seasonal and inter-annual patterns (Vargas et al., 2011b).

In general, these studies have concluded that the intense maintenance required by urban lawns can offset the carbon sequestration benefit provided by turfgrass. However, almost all studies have been conducted on lawns covered by cool-season grasses, such as Kentucky bluegrass (*Poa pratensis* L.), ryegrass (*Lolium* spp.) and fescue (*Festuca* spp.); species that tolerate and thrive under cold weather. The carbon dynamics of warm-season grasses, such as zoysia grass (*Zoysia* spp.) and Bermuda grass (*Cynodon* spp.) have been much less studied in subtropical locations, and to our knowledge, no study has been conducted in the tropics. Thus, the CO₂ flux in urban lawns covered by warm species such as cowgrass (*Axonopus compressus*), centipede grass (*Eremochloa ophiuroides*) and seashore paspalum (*Paspalum vaginatum*) has not yet been assessed. Guertal (2012) reviewed the research work done on the subject and highlighted the need of long-term studies over a greater variety of turfgrass species and climates to better assess the impact of management practices.

Warm-grasses are C₄ plants and are more efficient in fixing carbon than cool-grasses, which are C₃ plants. Grasses which utilize the C₄ photosynthetic pathway yield CO₂ assimilation rates 2–3 times higher than C₃ grasses, resulting in an increased biomass productivity (Waller and Lewis, 1979). Depending on several environmental and ecological factors (e.g., ambient temperature, solar irradiance, precipitation and soil characteristics), a higher productivity might represent a stronger carbon uptake, but also an increase of CO₂ emissions due to more frequent mowing. Thus, under constant hot and wet conditions that characterize tropical locations, warm grasses grow vigorously, making frequent mowing necessary, which in turn reduces the capacity of turfgrass to remove atmospheric CO₂.

To elucidate the potential role of turfgrass in the carbon cycle in tropical cities, the present study investigates the CO₂ exchange in a typical lawn of a residential neighborhood of Singapore. We hypothesize that urban lawns in the tropics might act as net sources of CO₂ to the atmosphere due to: a) warm and humid conditions that enhance F_s ; and b) the systematic use of mowing equipment, which in turn offset the amount of CO₂ assimilated by photosynthesis and stored in biomass and soil. Furthermore, from a management perspective, locally derived models for estimating carbon budgets related to F_s and biomass production are critical to mitigate potential environmental costs caused by maintaining aesthetic grounds. Thus, we test the performance of empirical models based on biophysical variables (e.g., soil temperature and moisture) to predict and evaluate monthly variations of both components using as reference the soil and grass characteristics of the studied lawn.

Results are expected to assist Singapore's efforts to improve the accounting of carbon fluxes and devise effective mitigation measures against climate change through an improved greenery management. The findings presented here may also help to design better programs to increase the environmental services provided by vegetation in tropical cities, where urbanization is projected to increase the most in the coming years (United Nations, 2018).

2. Methodology

A continuous and automated monitoring arrangement composed by two independent sets of flux-gradient systems was deployed over 35 months (Sept. 2014 to Jul. 2017) to measure F_s , production, and storage rate in an experimental plot in a private lawn of Singapore (1°18'51.46" N, 103°54'40.31" E; 5 m above sea level). These flux-gradient systems provided unprecedented high temporal resolution and were complemented with discrete manual F_s measurements to incorporate information regarding spatial variability. The carbon associated with biomass productivity aboveground was simultaneously evaluated by harvesting the clippings every time the turf was mowed. Singapore's lawns do not require irrigation thanks to frequent rainfall all year round. Although fertilization is a common practice in public lawns and parks (CUGE, 2010), no fertilizer was applied during the study, nor was there any application in the previous four years. The CO₂ emission related to mowing was estimated using emission factors and activity data.

Fig. 1 shows the components covered in this assessment: soil CO₂ efflux (F_s) including autotrophic and heterotrophic belowground contributions, amount of CO₂ produced (P_s) and stored in the soil (S_s), CO₂ removed by photosynthesis and stored by aboveground biomass, and CO₂ emissions from maintenance activities. The carbon removed by photosynthesis and allocated to belowground biomass production (i.e., roots, endophytes and mycorrhizal associations) is missing, as well as the autotrophic respiration of grass shoots (i.e., aboveground autotrophic respiration). We assume a negligible increase in roots biomass in the mature turfgrass, as well as a minimum CO₂ contribution from uncounted processes such as seeds production, and emission of volatile organic compounds and methane that constitute part of the net ecosystem carbon balance (NECB, Chapin et al., 2006), but are difficult to measure and often ignored in carbon budgets. The fate of the carbon stored belowground through time was not investigated in this study, it could accumulate in the lawn or loss by leaching as indicated in Fig. 1.

The amount of CO₂ assimilated by photosynthesis that returns to the atmosphere by autotrophic respiration (below and above ground) can be omitted from the NECB for timescales of days or longer. In short stature plants, the carbon assimilated by photosynthesis is quickly respired or rapidly transferred belowground and contributes to F_s (i.e., a few hours; Bahn et al., 2009; Vargas et al., 2011a). In the case of heterotrophic respiration, the decomposition of organic matter occurs in longer timescale (i.e., months to years), but under steady-state conditions like in our system, in which the factors controlling microbial activity, such as temperature, moisture and supply of grass litter are relatively constant,

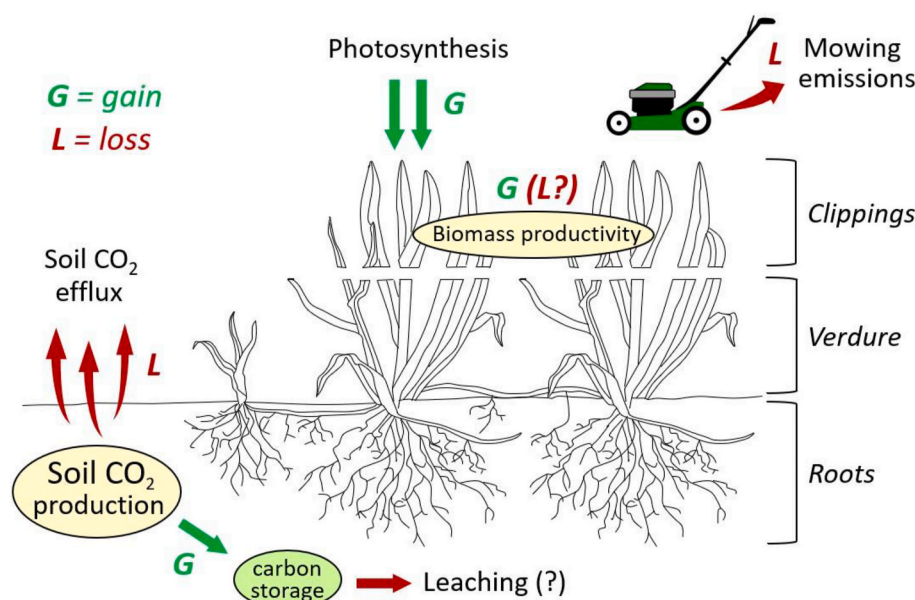


Fig. 1. Natural and anthropogenic components of the carbon dynamics (gains and losses) in an urban turf-grass system evaluated in this study: soil CO₂ efflux including heterotrophic and autotrophic respiration, soil CO₂ production and carbon storage, carbon uptake by photosynthesis and accumulation in grass biomass, and CO₂ emissions related to fossil fuel consumption for maintenance activities. As explained in the text, the carbon accumulated belowground could be loss through leaching. The grass sections showed here were analyzed for carbon content. Clippings, verdure and roots showed a carbon content of 43.2 ± 0.6, 41.2 ± 0.9 and 42.6 ± 1.5%, respectively.

only minor rapid variations are expected. Therefore, the microbial contribution can be omitted from the NECB, especially if the organic matter originates from the CO₂ assimilated by the grass itself (i.e., no external input of organic matter). This assumption neglects the carbon supply by older sources and mineral soil, which usually have a minor contribution to F_s (Trumbore, 2006).

2.1. Singapore's climate

Singapore's climate is characterized by high-temperature, -relative humidity and -rainfall, and low average wind speed all year round. Ambient temperature ranged from 25°C in the early morning to 32°C in the afternoon during the study. Relative humidity was 85–90% in the early morning and remained above 60% during the rest of the day, rarely went below 50%. A mean annual rainfall of 3870 mm was recorded, registering precipitation 74% of the days. Rainstorms were usually convective and rarely lasted longer than 1–1.5 h. However, they were frequent and intense throughout the year. Winds were in general calm and followed the direction pattern dictated by the monsoon seasons and land/sea breezes. Details of the local meteorology during the study can be found in the Supplementary Material (SM; section 1).

2.2. Lawn and soil characteristics

The studied lawn has a size of 46 × 32 m and is covered by cowgrass (*Axonopus compressus*). Cowgrass is the most common turfgrass species in Singapore (Yee et al., 2019). This species is adapted to low fertility and acidic soils. Most of Singapore's soils are low in organic matter, are nitrogen deficient, and exhibit pH values of ~5 (Leitgeb et al., 2019; Ghosh et al., 2016). Although cowgrass has a low tolerance to traffic (wear tolerance + recuperative potential), and is considered a turfgrass of low quality due to its reduced shoot density, it is the preferred species for turfed landscapes in Singapore because of its low fertilization requirements and mowing frequency (CUGE, 2010). An average shoot density of 570 ± 160 shoots m⁻² was measured by counting *in-situ* the number of shoots within sixty 15 × 15 cm sampling plots across the experimental lawn. The lawn has been relatively undisturbed for five decades. No major construction work has been conducted on the area since the building was built in 1967.

A stratified random approach was followed to collect soil samples from 27 locations across the lawn at eight different depths, and

determine the soil characteristics listed in Table 1 down to a depth of 1.3 m, except for bulk density (ρ_b), which was only possible to measure at the top two layers. Based on the relative proportion of sand, silt and clay, silty loam was the dominant soil type in the top 30-cm layer. Details of the sampling approach and samples analysis are provided in SM 2.1.

2.3. Soil CO₂ efflux, production and storage rate measurements

Soil CO₂ efflux (F_s), P_s and S_s were measured by two flux-gradient systems built using solid-state CO₂ sensors as described in multiple studies (e.g., Vargas and Allen, 2008; Tang et al., 2003). These independent systems were installed 5 m apart within a 4 × 4 m experimental plot placed in the centre of the studied lawn (see Fig. SM4).

While a larger number of monitoring points would have better addressed the spatial and temporal heterogeneity of F_s , instrumentation and field work expenses would have significantly increased. As it is explained latter, to account for the variability in soil characteristics, mean values of concurrent readings from both flux-gradient systems were used to calculate F_s , while mean values of the soil parameters

Table 1

Vertical variation of soil composition, TOC, pH and ρ_b obtained from 27 sampling locations across the selected lawn. Values are geometric mean ± one standard deviation.

Depth (cm)	Sand (%)	Silt (%)	Clay (%)	TOC (%)	pH	ρ_b (g cm ⁻³)
0–5	16.5 ± 16.6	68.9 ± 14.1	4.8 ± 3.3	1.9 ± 0.3	5.08 ± 0.50	1.08 ± 0.09
	11.1 ± 11.7	75.1 ± 10.5	8.3 ± 3.6	1.6 ± 0.3	5.13 ± 0.46	1.18 ± 0.11
15–20	3.8 ± 22.1	73.7 ± 16.2	15.3 ± 16.0	0.9 ± 0.2	5.52 ± 0.55	–
	3.4 ± 22.1	63.8 ± 21.5	15.3 ± 15.8	0.5 ± 0.1	5.67 ± 0.47	–
25–30	46.5 ± 34.5	8.3 ± 28.6	4.1 ± 6.1	0.3 ± 0.1	5.74 ± 0.47	–
	98.7 ± 2.4	1.2 ± 2.2	0.1 ± 0.1	0.3 ± 0.2	5.72 ± 0.34	–
100–105	99.5 ± 1.5	0.5 ± 1.4	0.0 ± 0.1	0.4 ± 0.2	5.73 ± 0.33	–
	125–130	98.7 ± 2.4	0.0 ± 2.2	0.0 ± 0.1	0.4 ± 0.2	5.66 ± 0.36

needed to assess the soil diffusivity (i.e., soil texture and ρ_b) were obtained across the lawn. Automated soil CO₂ measurements provide unprecedented temporal resolution, but compromise spatial information (Cueva et al., 2017; Vargas et al., 2011b).

Under the assumption that molecular diffusion dominates the gas transport process in soil, the method calculates F_s (in $\mu\text{mol CO}_2 \text{ m}^{-2} \text{ s}^{-1}$) from CO₂ concentration measurements in the soil profile based on Fick's first law of diffusion:

$$F_s = -D_s \frac{\partial C}{\partial z} \quad (1)$$

where D_s is the gaseous diffusion coefficient of CO₂ in soil (i.e., soil CO₂ diffusivity in $\text{m}^2 \text{ s}^{-1}$) and $\partial C/\partial z$ is the rate of change of the molar CO₂ concentration (in $\mu\text{mol m}^{-3}$) with depth (z in m).

Standardized measurement and postprocessing methods were followed in this study (Tang et al. 2003, 2005; Vargas et al., 2010). Briefly, for each flux-gradient system, three solid-state CO₂ sensors (range 01–10000 ppm model GMT 222, Vaisala, Finland; accuracy: $\pm 1.5\%$ of the range and +2 of reading) and three soil temperature (T_s) and volumetric water content (Θ_s) sensors (5TM, Decagon Inc., Pullman, USA; resolution, accuracy: 0.1°C , $\pm 0.3^\circ\text{C}$; $0.001 \text{ m}^3 \text{ m}^{-3}$, $\pm 3\%$) were installed at 2, 8 and 16 cm of depth as shown in the sketch of Fig. SM4. The CO₂ sensors were calibrated at the beginning, middle and end of the study with zero air and three gas mixtures (Scott-Marrin Inc. Standard 337, 531 ppm and 2788 ppmv, National Institute of Standards and Technology). Data were recorded continuously every 5 min. Soil CO₂ concentrations were corrected for temperature and pressure according to the manufacturer, and passed through a Savitzky-Golay smoothing filter to reduce noise that could affect the postprocessing of F_s and P_s .

The CO₂ diffusivity was calculated as a function of Θ_s , percentage of mineral soil with size $>2 \mu\text{m}$, which represents the sum of silt and sand content ($S = \text{silt} + \text{sand}$), and soil porosity according to Moldrup et al. (1999), and corrected for pressure and T_s . The steps followed to estimate D_s are described in detail in SM-3.2.

Assuming a constant rate of CO₂ production in the upper part of the soil profile (i.e., 2 cm depth), F_s was calculated as follow using 30-min mean data obtained from the 5-min readings delivered by the instruments:

$$F_s = \frac{z_{i+1}F_i - z_iF_{i+1}}{z_{i+1} - z_i} \quad (2)$$

where F_s , F_i and F_{i+1} are CO₂ effluxes at depths z_0 , z_i and z_{i+1} , respectively. Once F_i is calculated for each depth in the soil profile ($z_0 = 2 \text{ cm}$, $z_i = 8 \text{ cm}$ and $z_{i+1} = 16 \text{ cm}$), P_s is calculated from the difference between the effluxes across adjacent depths as a flux divergence:

$$P_s = \frac{F_i - F_{i+1}}{z_{i+1} - z_i} \quad (3)$$

where P_s is the rate of soil CO₂ production (in $\mu\text{mol m}^{-3} \text{ s}^{-1}$) in the soil layer between depths i and $i+1$.

The difference between P_s and F_s defines S_s . A sustained positive difference indicates that more carbon is transferred from turfgrass to topsoil than released by F_s , and therefore soil acts as a CO₂ storage pool under steady state conditions.

A soil chamber (LI-8100A, Li-COR, Lincoln, USA) was used to compare and adjust the F_s obtained from the flux-gradient method. Soil chamber F_s measurements are not without uncertainties. The chamber and grass clipping within the collard alter the microenvironment, as well as the soil gas flux. However, these uncertainties are expected to be lower than those associated with the estimates of D_s , especially in conditions close to water saturation, as frequently experienced in the studied lawn (see Maier and Schack-Kirchner, 2014). During a 4.5-month period, 180 manual chamber measurements were made during daytime (between 7 and 18 h) in four permanent locations (i.e., soil rings) installed within the experimental plot (see Fig. SM4). As a

common practice, aboveground grass biomass within the soil rings was removed by clipping at the soil surface to avoid including leaf respiration. Autotrophic respiration from adjacent roots that extended underneath is expected to contribute to total F_s . Each measurement lasted 2 min, and F_s was obtained using the LI-1800 software. Readings with a regression coefficient <0.9 were rejected and represented 3% of the total observations.

The flux-gradient method had a satisfactory agreement with the soil chamber method ($r^2 = 0.58$), despite the spatial heterogeneity of these manual measurements. Comparisons between both methods in natural terrestrial ecosystems have reported correlation coefficients ranging from 0.50 to 0.95 (see Table 1 in Maier and Schack-Kirchner, 2014). A scatter plot between both methods is presented in Fig. SM5.

2.4. Soil CO₂ efflux modeling

With the aim of developing a simple model to estimate the F_s contribution to the atmosphere in the neighborhood housing the lawn, we tested the influence of T_s and Θ_s as independent variables to predict the F_s variability. We followed the exponential relationship applied previously by authors who have also used the flux-gradient method (Tang et al., 2005; Vargas and Allen, 2008):

$$F_s = \beta_0 e^{\beta_1 T_s} e^{\beta_2 \Theta_s + \beta_3 \Theta_s^2} \quad (4)$$

the model coefficients β_0 , β_1 , β_2 and β_3 were estimated from the entire time series using the Curve Fitting application of IGOR Pro 7. Mean values of T_s and Θ_s from the three measurement depths were used for the fitting analysis.

We also evaluated the capability of the empirical Q_{10} model based on van't Hoff equation to simulate F_s . This model assumes that F_s responds only to T_s changes in the absence of Θ_s limitations:

$$F_s = R_{10} Q_{10}^{\frac{T_s - 10}{10}} \quad (5)$$

R_{10} is the specific respiration rate at 10°C and Q_{10} the increase in respiration rate per 10°C rise in T_s . The almost universal Q_{10} value of $1.4 \pm 0.1 \mu\text{mol m}^{-2} \text{ s}^{-1}$ across climate zones and ecosystems proposed by Mahecha et al. (2010) was applied, while a site specific R_{10} was obtained from the T_s data collected at the 8 cm depth.

The performance of both models was evaluated by the mean relative error (ϵ), mean bias (*Bias*), and coefficient of variance (*CV*). The former is the relative difference between estimated ($F_{s \text{ est}}$) and observed ($F_{s \text{ obs}}$) values. The mean bias evaluates the model's systematic error, while *CV* evaluates the total error, including random errors. The former two metrics provide insight on the model uncertainty to estimate the long-term mean, while *CV* gives insight on the errors for individual estimations. For the purpose of this study, a relatively large value of *CV* can be acceptable as long as the *Bias* is low, since errors at individual level tend to cancel out. These three metrics are defined as:

$$\epsilon = 100\% \times \frac{1}{N} \sum_{i=1}^N \left(\frac{F_{s \text{ est}}(i) - F_{s \text{ obs}}(i)}{F_{s \text{ obs}}(i)} \right) \quad (6)$$

$$\text{Bias} = 100\% \times \frac{\sum_{i=1}^N (F_{s \text{ est}}(i) - F_{s \text{ obs}}(i))}{\sum_{i=1}^N F_{s \text{ obs}}(i)} \quad (7)$$

$$\text{CV} = 100\% \times \frac{\left(\frac{1}{N-k} \sum_{i=1}^N (F_{s \text{ obs}}(i) - F_{s \text{ est}}(i))^2 \right)^{\frac{1}{2}}}{\frac{1}{N} \sum_{i=1}^N F_{s \text{ obs}}(i)} \quad (8)$$

where N and k are the number of readings and number of independent variables, respectively.

2.5. Turfgrass's net biomass productivity measurements and modeling

To evaluate the carbon assimilated by photosynthesis and stored in grass shoots, the biomass productivity aboveground was measured by harvesting and weighting grass clippings. Clippings from a 4 m² area adjacent to the experimental plot (see Fig. SM4) were collected every time the turf was mowed, at least once per month. Clippings were harvested by a rake first and then collected using a portable vacuum. The common practice in Singapore is to remove clippings after mowing, since they are considered unsightly.

Thirty-five harvested clipping samples were collected during the study. Clippings were dried at 60°C for 72 h in an oven, and then weighted using an electronic balance with an accuracy of 0.1 g. The clippings' dry weight was then converted to carbon mass using a carbon content of 43.20%.

The carbon content in grass clippings, verdure or stubble, and roots was determined at the beginning of the study (see Fig. 1). Samples were collected from three plots of 50 × 50 cm across the lawn. Each grass component was individually analyzed. Verdure and roots were hand washed and sieved with a 0.25 mm² mesh size. Live and dead roots were separated by testing for flotation and root color. After drying, the samples were grinded to a particle size <63 μm using a ball mill. The total carbon content was determined using a TOC analyzer (Vario TOC Cube, Elementar Analysensysteme GmbH).

An empirical model was developed to estimate the turfgrass aboveground biomass productivity as a function of plant-available soil water. The soil water potential due to moisture tension (Ψ_{θ}) was used as a proxy of plant-available soil water (Or and Wraith, 2002). Ψ_{θ} was obtained from the soil water retention curve derived from the Saxton and Rawls (2006) equations using as input information the soil texture characteristics and organic matter content from the 10-cm upper layer. To accommodate local variations of soil density, a density adjustment factor (DF = 0.743) was incorporated to estimate Ψ_{θ} . The resulting curve ($\Psi_{\theta} = 1.60\Theta_s^{-2.56}$) can be found in Fig. SM6. For each harvesting period a mean Ψ_{θ} value was obtained from the 5-min Θ_s data collected by both flux-gradient systems at a depth of 2 cm.

2.6. Estimation of CO₂ emissions from mowing

Emissions of CO₂ related to mowing were estimated using emission factors and activity data. Emission factors were obtained from the United States Environmental Protection Agency (EPA) Motor Vehicle Emission Simulator (MOVES) version 2014b (USA-EPA, 2018). MOVES is a state-of-the-art emission modeling system that estimates emissions of both, on-road vehicles and non-road equipment. The latter includes gasoline-powered lawn and garden equipment, ranging from string trimmers to small tractors. MOVES accounts for the altitude and climate characteristics but is limited to locations in the United States of America. Thus, emission factors for Miami, Florida estimated for the summer months were used as a proxy of Singapore's emission factors.

MOVES yields emission factors as a function of time (i.e., CO₂ grams per hour of mowing). For our purpose the factors were converted to emissions per unit of mowed area. Equipment manufacturers provide formulas like the following to calculate how long it will take to mow a specific area according to the equipment's engine and deck/cutting width (e.g., Encore Power Equipment, <http://www.encoreequipment.com>):

$$\text{Mowing time} = \frac{108.9 \times \text{Area}}{\text{Speed} \times 0.9 \times \text{Deck width}} \quad (9)$$

where the area to mow is in acres, the recommended mowing speed in mph, the deck width in inches, and the resulting mowing time in hours. Note that Imperial units are still the customary units in landscaping management. The factor 108.9 includes the acres per hour dimensions and a 10% time-factor for turning at the ends of swaths. The manufac-

turer recommends using a 9/10 of the mower deck width to factor in overlapping swaths for a uniform mowing job. For string trimmers, we took as reference the mean speed of 9.13 s to trim a plot of 5 × 5 ft (11.11 h ha⁻¹) obtained from an evaluation of 10 commercial trimmers (Johnson, 2018).

To obtain insight of the emissions range yield by the variety of mowing equipment available in the market, we assessed the CO₂ emissions of sixteen gardening machinery, including backpack trimmers, push mowers, riding mowers and lawn tractors. Their characteristics and emission factors per unit of mowed area are presented in Table SM3.

3. Results

The time series of all variables associated with the carbon dynamics of turfgrass systems evaluated in this study are presented and described in this section, together with the resulting carbon stored in soil and grass biomass, and emissions from fossil fuel consumption associated to maintenance activities. The performance of the proposed models is also evaluated as part of the results section.

No seasonal trend is observed in the time series of F_s , P_s and S_s , as well as in the environmental variables on which they depend as shown in Fig. 2. Monthly variations of P_s and S_s were more evident than those of F_s , as depicted by Fig. 3. Low monthly values were apparently triggered by scanty rainfall. Fig. 4 shows that the diurnal variability of F_s responds to changes in T_s in a soil permanently wet, while the two-month closeup of Fig. 5 illustrates the impact of downpours in F_s along with the limitations of empirical models to reproduce such episodes. The same figure shows the models ability to reproduce the diurnal variability and trend along several days. Similarly, Fig. 6 shows that the proposed exponential correlation to estimate the aboveground biomass productivity using Ψ_{θ} as a proxy of plant-available soil water can reproduce the annual mean, as well as the monthly values, but with a lower accuracy.

3.1. Carbon stored in soil and grass biomass

A mean soil carbon concentration and density of 35 ± 6 g C kg⁻¹ and 1.97 ± 0.38 kg C m⁻² were obtained for topsoil (i.e., 10-cm top layer) based on the TOC and ρ_b data collected from the two upper depths sampled across the entire lawn. Turfgrass adds 0.27 ± 0.06 kg C m⁻² all year long, of which 12.2%, 52.6% and 35.2% are contained in clippings, verdure and living roots. In total, topsoil and grass store together 2.24 ± 0.44 kg C m⁻².

The topsoil's silty loam texture, low TOC content (1.5–2.5%), moderately acidic pH (5.10–5.15) and slightly below optimal ρ_b (1.00–1.20 g cm⁻³) are common characteristics of Singapore's soils, to which the resistant cowgrass adapts well. The *kampong* (Malay fishing village) origin of the site explains the high and consistent proportion (>95%) of sand, and constant pH of ~5.5 and TOC of ~0.5% at depths bellow 50 cm (see Table 1).

3.2. Soil CO₂ efflux

The tropical weather of Singapore sustains warm and wet conditions favorable to constant F_s all year long. The 16-cm upper layer of the studied lawn never showed temperatures <25°C, neither became dry as Θ_s rarely was below 0.15 m³ m⁻³. Frequent downpours triggered Θ_s spikes up to 0.3–0.4 m³ m⁻³, driving T_s fluctuations of 4–5°C at the upper layer. The variability of these two parameters decreased considerably at 8 and 16 cm (see Fig. 2c and d).

Both flux gradient systems yielded similar magnitudes, variability and trends for T_s and Θ_s at the three monitored depths. Variability and trends for CO₂ concentrations were also similar, but system #2 recorded regularly higher values. Differences of 15%, 38% and 18% for individual readings at depths of 2, 8 and 16 cm drove a consistent 35% difference in F_s . This difference could respond to the variability in soil texture, TOC and soil porosity across the lawn, as well as variations in P_s . To account

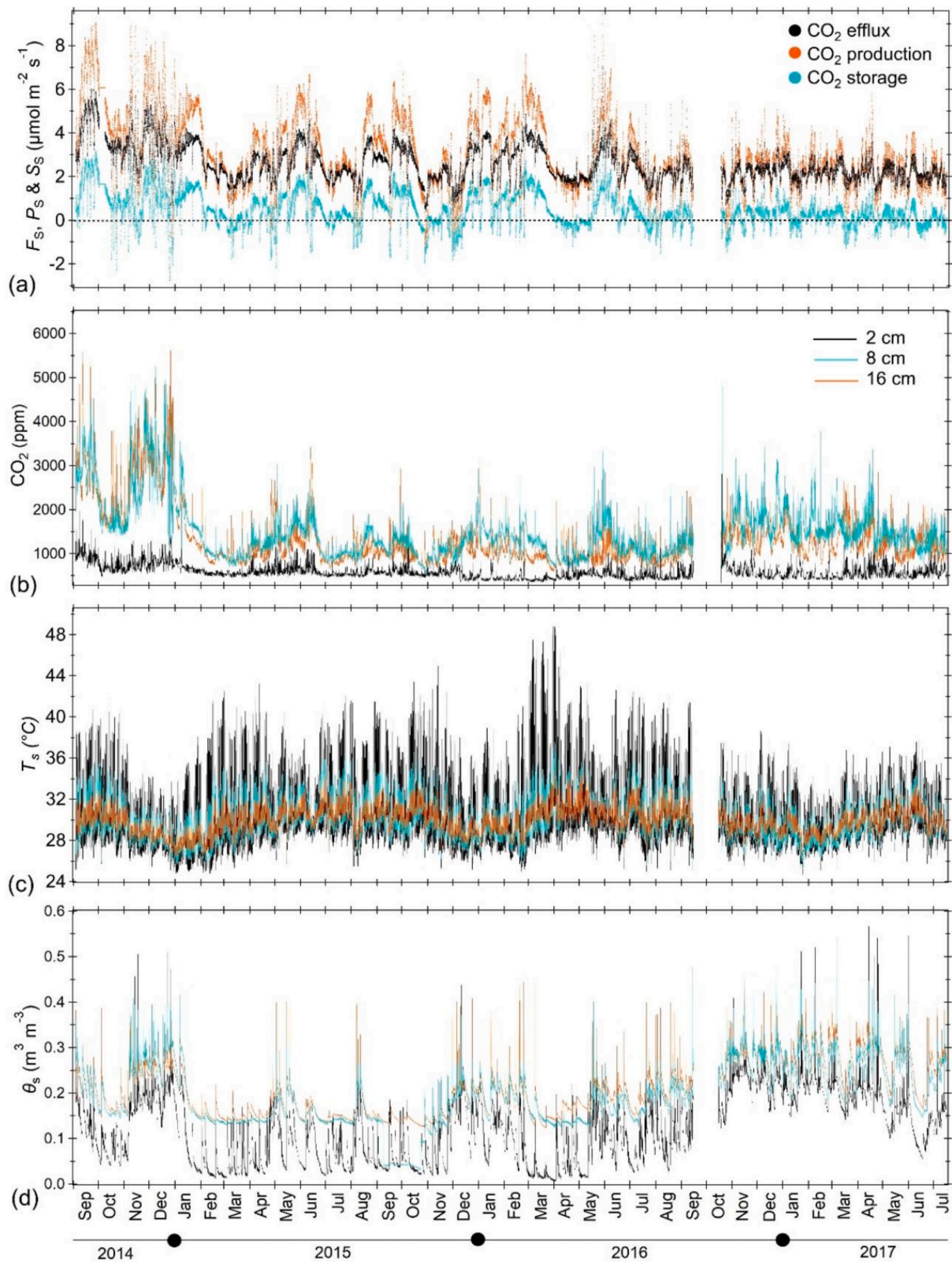


Fig. 2. Time series of soil CO₂ efflux (F_s), production (P_s) and storage (S_s) rates (a), soil CO₂ concentration (b), soil temperature (T_s , c) and volumetric soil moisture (θ_s , d) along the entire study. Soil CO₂ efflux was computed using mean 30-min values of T_s , θ_s and CO₂ concentration of concurrent readings from the two flux gradient systems installed in the centre of the studied lawn. T_s , θ_s and CO₂ concentration were measured every 5 min at depths of 2, 8 and 16 cm as explained in the text. Soil CO₂ production and storage rate cover the 16-cm upper layer.

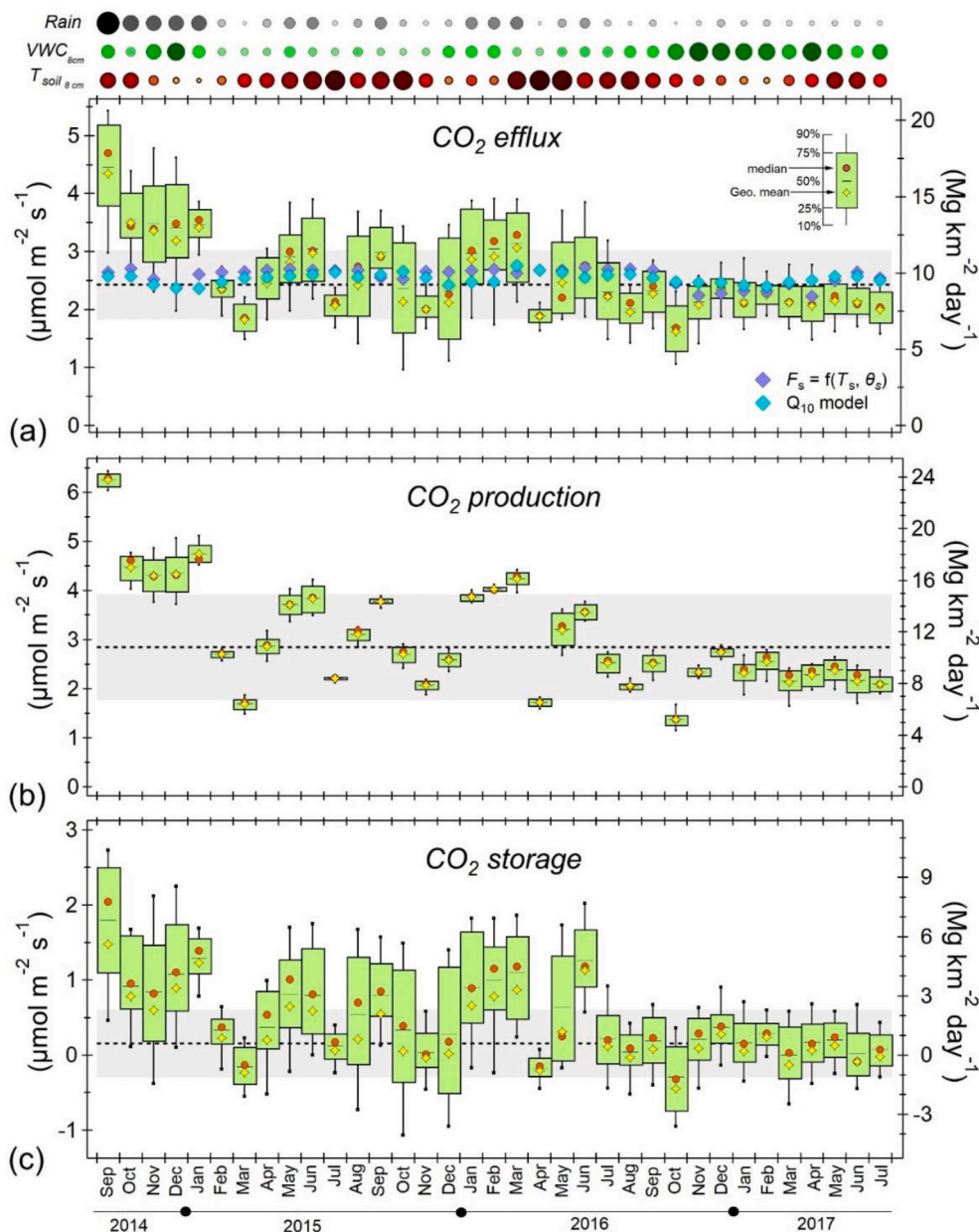


Fig. 3. Monthly variations of soil CO_2 efflux (a) production (b) and storage rate within the 16 cm upper layer along the 35 months covered by this study. The horizontal dashed lines indicate long-term means, while the gray shades are ± 1 standard deviation from such means and give an indication of the month-to-month variability. The colored circles at the top provide insight of the monthly variability in rainfall, θ_s and T_s at 8 cm of depth. Larger circles and intense colors indicate higher values. (For interpretation of the references to color in this figure legend, the reader is referred to the Web version of this article.)

for this inherent issue and obtain a more representative F_s estimation, mean values of concurrent readings from both systems were used for the efflux data postprocessing.

No seasonal variations were observed, but two periods displayed slightly different trends (see Fig. 3). The first four weeks of the study overlapped with the inter-monsoon period and were marked by scanty rainfall, contrary to the next eight weeks that marked the beginning of the rainy Northeast monsoon. The highest mean F_s , $4.35 \pm 0.91 \mu\text{mol m}^{-2} \text{s}^{-1}$, was recorded during the first two weeks of measurements in Sep. 2015 and responded to a high P_s , which in turn was reflected by high CO_2 concentrations at the three measurement depths. The next four months registered mean F_s ranging from 3.18 to $3.50 \mu\text{mol m}^{-2} \text{s}^{-1}$, values well above the study average of $2.43 \pm 0.58 \mu\text{mol m}^{-2} \text{s}^{-1}$ ($281 \pm 68 \text{ Mg CO}_2 \text{ km}^{-2} \text{ month}^{-1}$, $77 \pm 18 \text{ Mg C km}^{-2} \text{ month}^{-1}$). October 2015 accumulated the second lowest amount of rainfall throughout the study, 11 mm, but Nov. and Dec. of that year recorded the highest, 69 and 86 mm, respectively. During those months, P_s was intense under a soil with abundant moisture and slightly less warm.

The F_s during the rest of the study was within the expected variability of ± 1 standard deviation from the geometric mean. Only Feb. 2016 and Oct. 2016 showed monthly F_s means slightly above ($3.07 \pm 0.65 \mu\text{mol m}^{-2} \text{s}^{-1}$) and below ($1.62 \pm 0.52 \mu\text{mol m}^{-2} \text{s}^{-1}$) that range, respectively.

In terms of diurnal variability, frequent rainfall hinders a clear F_s pattern. Although rain is more often during daytime, it can be expected at any time (Mandapaka and Qin, 2013). To draw a consistent diurnal pattern in days not affected by rainfall, we analyzed the last nine months of the study, when F_s was less variable. As depicted in Fig. 4, F_s depends apparently on T_s , but not on θ_s . F_s was high at night, fell sharply in the morning and increased again in the afternoon. The minimum value was attained before noon, 2 h after the coolest time of the day.

3.2.1. Performance of soil CO_2 efflux models

As shown in Fig. 3, both proposed models based on 30-min data reproduced the monthly means of F_s within a reasonable uncertainty ($\epsilon < 13.5\%$ and $\text{Bias} < 1.5\%$), but not individual readings at such fine temporal resolution, neither captured faithfully the daily variability.

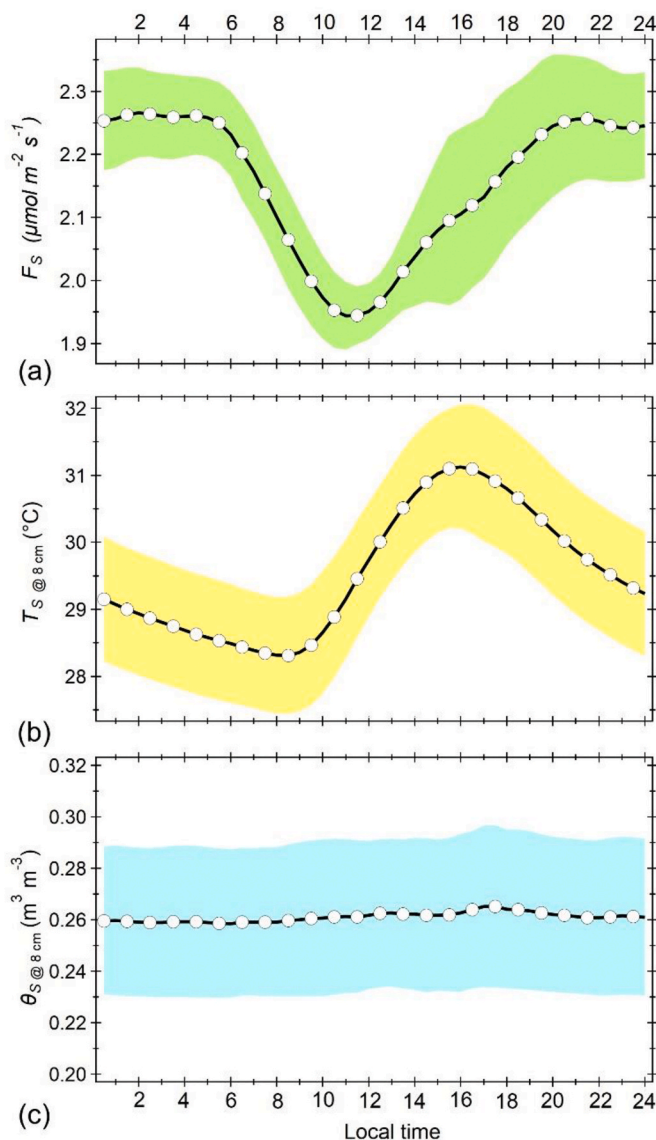


Fig. 4. Mean diurnal variations of F_s (a), T_s (b) and Θ_s (c) at 8 cm of depth during the Jan.-Jul. 2017 period. T_s and Θ_s data at 8 cm of depth showed less noise than at 2 cm, and diurnal differences in T_s were larger than at 16 cm. The colored shaded areas are ± 1 standard deviation from the means and give an indication of the day-to-day variability at every hour of the day.

The exponential correlation based on T_s and Θ_s (eq. (4), $\beta_0 = 1.853$, $\beta_1 = 0.001$, $\beta_2 = 4.608$, and $\beta_3 = -14.761$) and the Q_{10} model (eq. (5), $R_{10} = 1.31$) yielded essentially the same uncertainty for simulating 30-min values. The former model yielded a CV of 32.1%, while the latter of 34.6% when using the entire dataset. However, since the aim is to estimate the annual F_s , the relatively large CV can be acceptable, since the *Bias* is low. Fitting both models to daily values did not improve the performance. The long-term evaluation metrics decreased somewhat ($\epsilon < 7.6\%$ and *Bias* $< 0.15\%$), but not the prediction on a daily basis (CV $< 31.0\%$).

The exponential correlation obtained from the 30-min data reproduced the tendency through several days, as well as the negative spikes caused by intense rainfalls, but not the diurnal pattern as shown in Fig. 5. The Q_{10} model reproduced the diurnal pattern with a consistent delay of ~ 3 h in the maximum and minimum values, but failed to reproduce the trend across multiple days, and could not model sudden drops caused by downpours that rapidly reduce soil CO_2 diffusion rates.

In terms of T_s and Θ_s data at different depths, no significant difference was found using average data from the three depths ($\epsilon = 13.2$, *Bias* = -0.15 , CV = 32.1) and data from the sensors installed at the 2 cm depth ($\epsilon = 13.4$, *Bias* = 0.4, CV = 31.8) for the exponential correlation considering the entire dataset. Similarly, no difference was observed using T_s data at a depth of 8 cm ($\epsilon = 15.0$, *Bias* = 0.9, CV = 34.6) and at a depth of 2 cm ($\epsilon = 12.5$, *Bias* = 1.2, CV = 34.7) for the Q_{10} model.

3.3. Soil CO_2 production and storage belowground

The P_s and storage rate within the 16-cm upper layer showed, as expected, the same pattern and trend of F_s (see Fig. 2a). The following linear correlations reproduce the observed P_s and S_s as function of F_s within uncertainties $< 2.5\%$ and $< 12\%$, respectively.

$$P_s = 1.87F_s - 1.78, r^2 = 0.98 \quad (10)$$

$$S_s = 0.87F_s - 1.78, r^2 = 0.91 \quad (11)$$

Fig. 3b shows the monthly variations of P_s and S_s . Monthly P_s means ranged from 1.38 to 6.25 $\mu\text{mol m}^{-2} \text{s}^{-1}$ with an overall mean of $3.05 \pm 1.60 \mu\text{mol m}^{-2} \text{s}^{-1}$.

With respect to S_s , on average $652 \pm 1068 \text{ Mg CO}_2 \text{ km}^{-2} \text{ yr}^{-1}$ were stored under the three years study. Monthly values ranged from -33 to $205 \text{ Mg CO}_2 \text{ km}^{-2} \text{ month}^{-1}$. Negative values (i.e., loss of carbon already stored) were recorded in 28% of the 30-min averaging periods. There were three months with zero carbon storage. March 2015, Apr. 2016 and Oct. 2016 recorded losses ranging from 18 to 33 $\text{Mg CO}_2 \text{ km}^{-2} \text{ month}^{-1}$. The lowest F_s and P_s values were also recorded in these months, and were apparently related to low Θ_s and scarce precipitation during the previous 30 days.

3.4. Turfgrass's aboveground biomass productivity

A mean turfgrass biomass productivity aboveground of $1059 \pm 394 \text{ Mg km}^{-2} \text{ yr}^{-1}$ ($1671 \pm 624 \text{ Mg CO}_2 \text{ km}^{-2} \text{ yr}^{-1}$) was determined under the three-year study. All biomass productivity amounts are expressed in units of dry-weight, otherwise is indicated. Monthly values ranged from 22.9 to 157.5 $\text{Mg km}^{-2} \text{ month}^{-1}$ following an inverse trend to the mean monthly values of Ψ_0 used as a proxy of plant-available soil water. High values of Ψ_0 indicate a lack of plant-available soil water, and *vice versa*. Thus, periods of high biomass productivity presented low values of Ψ_0 and were characterized by intense and frequent precipitation. For example, the large volume of rainfall accumulated between Nov. 2014 and early Jan. 2015 triggered low values of Ψ_0 and favored biomass productivity (see Fig. 6a). The largest clippings harvesting was at the end of such period. In contrast, the following three months were characterized by little rainfall, high Ψ_0 values and low biomass productivity.

Although some periods as those described above were present during the study, similar to F_s , the biomass productivity showed none seasonal trend. The perennially wet soil always sustained green grass and intense F_s . According to our observations, the biomass productivity aboveground in non-irrigated urban lawns covered by cowgrass in Singapore ranges from 2 to 3.5 $\text{g m}^{-2} \text{ day}^{-1}$ all year long. This intense biomass productivity forces a frequent mowing regime. In highly managed gardens, cowgrass is mowed every 6–9 days to keep an aesthetic turfgrass (CUGE, 2010). In residential lawns like ours, the mowing can be less frequent while a grass height of 5–6 cm is maintained to keep a healthy turf.

3.4.1. Performance of proposed model for aboveground biomass productivity

The proposed exponential correlation to estimate the aboveground biomass productivity as a function of Ψ_0 , and therefore Θ_s , was able to reproduce the annual biomass productivity within a deviation $< 3\%$. However, estimates at monthly scale were less accurate. Although the correlation captured the monthly trend, it consistently underpredicted

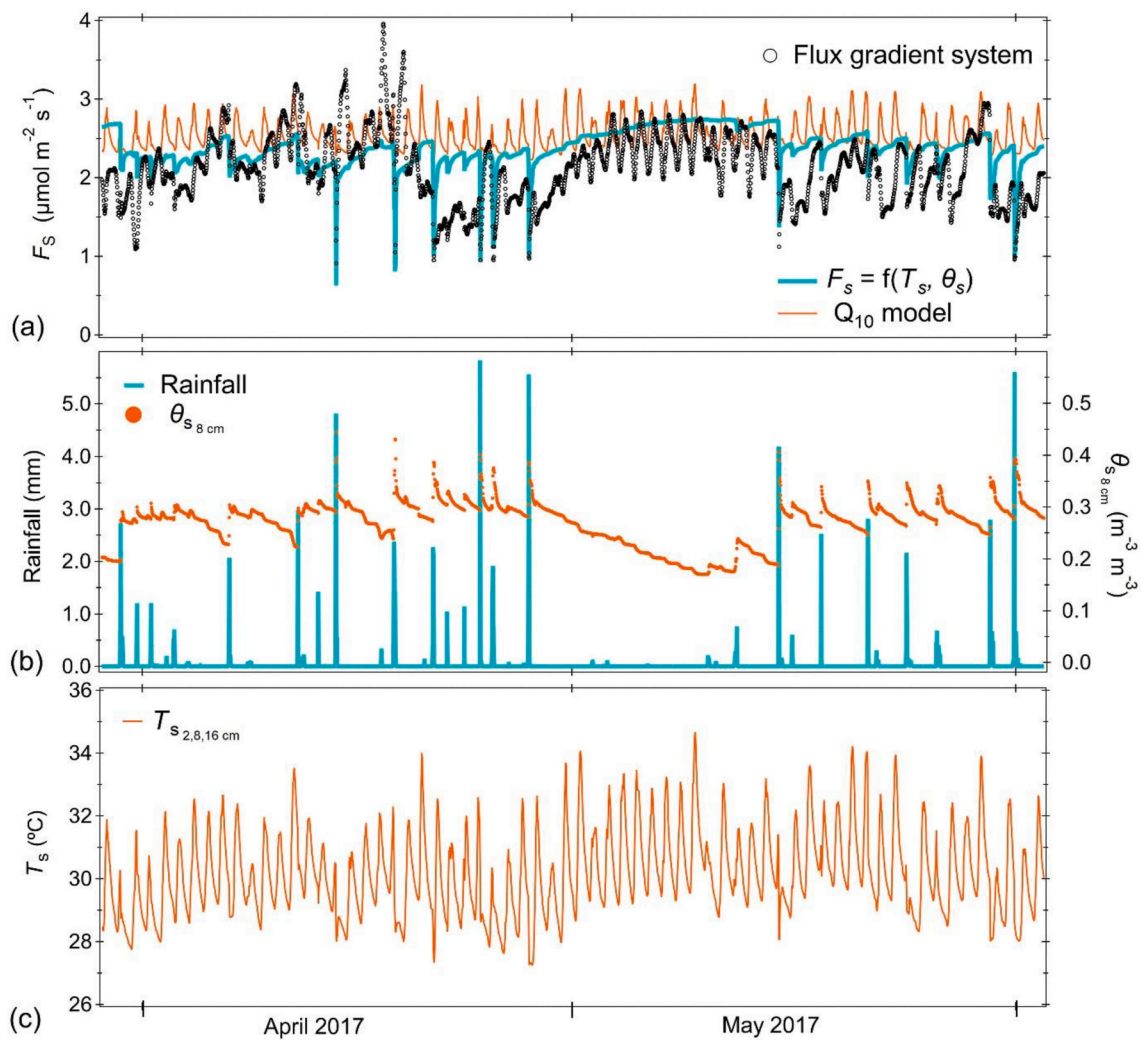


Fig. 5. Time series of F_s (a), rainfall and θ_s at 8 cm of depth (b), and T_s across the 16 cm upper layer (c) covering two months of measurements. Panel (a) includes modelled and measured soil respiration data.

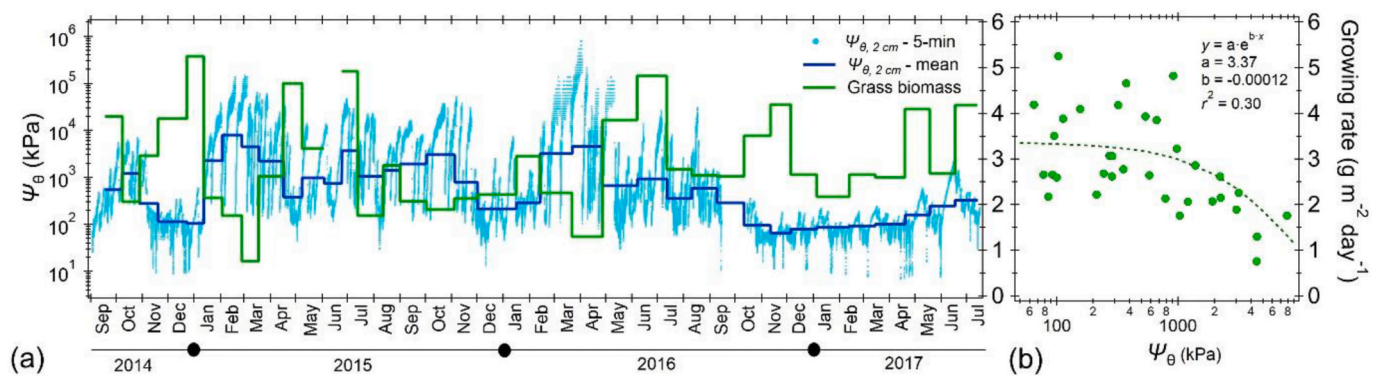


Fig. 6. Time series of turfgrass aboveground biomass productivity along with soil water potential due to moisture tension (Ψ_θ) as a proxy of plant-available soil water (a). Ψ_θ was obtained from θ_s readings at 2 cm of depth and a soil water retention curve derived for the specific soil texture and organic content matter at the studied lawn. The exponential regression that best fits both variables is shown in (b).

spikes of over $100 \text{ Mg dry-weight km}^{-2} \text{ month}^{-1}$. The moderate correlation coefficient of 0.30 displayed for the periodic clipping harvest (see Fig. 6b) responded to the variability in soil characteristics and grass shoots' density across the studied plot, as well as variations in the grass mowing and clippings collection, which altogether yielded a minor deviation after one year of sampling.

3.5. Mowing emissions

Depending on the mowing frequency and mowing equipment, CO_2 emissions from fossil fuel consumption used to maintain an aesthetic turf range from 6.5 to $78.2 \text{ Mg CO}_2 \text{ km}^{-2} \text{ yr}^{-1}$. Fig. 7 tabulates the emissions obtained for a representative set of commercially available mowers and

trimmers as a function of mowing frequency. Rear engine riding mowers are the most efficient equipment in terms of mowing productivity ($<1 \text{ h ha}^{-1}$) and CO_2 emissions per mowed area ($<7 \text{ kg CO}_2 \text{ ha}^{-1}$). These mowers are usually equipped with four-stroke engines of at least 20 HP, whose high emission rate ($>7200 \text{ g CO}_2 \text{ h}^{-1}$) is offset by wide cutting blades (>50 inches) and fast mowing speeds (7–12 mph). Mowing performance depends on the mowing speed and size of the spinning blades, which in turn set the engine's capacity. Emission factors for other types of mowers range from 9 to $16 \text{ kg CO}_2 \text{ ha}^{-1}$. Backpack trimmers are the least expensive mowing equipment, but their cutting efficiency is the lowest (11 h ha^{-1}) because of their small engine (≤ 2 HP) and mowing speed set by the gardener's walking pace, which altogether yield emissions of $15 \text{ kg CO}_2 \text{ ha}^{-1}$.

A turfgrass mowed once per week using a backpack trimmer releases $78.2 \text{ Mg CO}_2 \text{ km}^{-2} \text{ yr}^{-1}$ to the atmosphere, but if the mowing frequency is reduced to once per month, the associated CO_2 emissions drop to $18.0 \text{ Mg CO}_2 \text{ km}^{-2} \text{ yr}^{-1}$. Similarly, in case of using a push mower the emissions decrease from 82.6 to $19.1 \text{ Mg CO}_2 \text{ km}^{-2} \text{ yr}^{-1}$, and using a rear engine riding mower from 28.0 to $6.5 \text{ Mg CO}_2 \text{ km}^{-2} \text{ yr}^{-1}$.

Push mowers are the most common mowers used by Singapore's dwellers to manage their backyards, while a combination of riding mowers, lawn tractors and trimmers are used to manage public parks and road verges. Based on the gardening management observed in our lawn, we adopted a push mower equipped with a four-stroke engine of 5 HP, whose mowing speed yields an efficiency of 9.6 h ha^{-1} , to estimate the CO_2 emissions associated with turfgrass maintenance in residential lawns. Assuming a 3-weeks mowing frequency regime, an annual CO_2 emission of $27.0 \text{ Mg CO}_2 \text{ km}^{-2} \text{ yr}^{-1}$ was obtained.

4. Discussion

First, we compared the annual rates of F_s and aboveground biomass productivity at our study site with other grassland systems. Secondly, the net carbon flux budget (obtained by adding the contribution of each flux component) is scaled to neighborhood and city scales considering the fraction of surface covered by turfgrass, and assuming similar characteristics. Thirdly, we further discuss the challenges to empirically simulate the responses of F_s to main environmental factors in tropical urban settings.

4.1. Soil CO_2 efflux rate as compared to other grassland systems

Table 2 shows annual F_s for natural, managed and unmanaged rural, and urban grassland systems. For the former three types of grasslands, mean values were obtained from rates listed by the Global Soil Respiration Database (GSRD; Bond-Lamberty and Thomson, 2018). Based on such rates, the mean F_s ($3370 \pm 812 \text{ Mg CO}_2 \text{ km}^{-2} \text{ yr}^{-1}$) from our tropical urban lawn is in general higher than those reported for natural grasslands in tropical, subtropical and Mediterranean, and temperate regions. That said, our results are within the range (and associated uncertainty) of the modelled annual F_s for all grasslands around the world (Warner et al., 2019). Unmanaged grasslands present higher annual rates in tropical, and subtropical and Mediterranean zones, and somewhat lower or similar in temperate locations. Compared to managed grasslands in subtropical, Mediterranean, and temperate regions, our F_s were similar or slightly higher based on data from the GSRD.

There is limited information for managed tropical grasslands. Data are only available for a rural grassland in Singapore covered by cowgrass, like our lawn, and exposed to minimal management (i.e., infrequent mowing, no irrigation and no fertilization; Ng et al., 2015). The interpolated annual mean F_s from such data collected by periodic flux chamber measurements during a 5-month period exceeds 2.9 times the mean rate at our residential lawn. A higher TOC (5.45%), lower ρ_b (0.80) and different soil texture (clay loam) may explain the difference, but a systematic bias caused by measurements frequency and limitation to daytime hours cannot be neglected (Cueva et al., 2017).

For urban lawns, we can only compare our results to a limited number of studies in subtropical and temperate cities. In both cases, F_s can exceed by a factor >3 the mean F_s of our lawn, as shown in Table 2 for turfgrasses of Phoenix and Fort Collins, USA, and Moscow, Russia. These F_s were obtained from manual flux chamber measurements on selected days during daytime like Ng et al. (2015), and may not be comparable to diurnal and seasonal rates, besides that do not account for episodic events, such as downpours that influence the response of F_s resulting in pulse events that substantially increase annual rates (Kim et al., 2012).

4.2. Aboveground biomass productivity as compared to other grassland systems

The aboveground biomass productivity of the turfgrass studied here ($1059 \pm 394 \text{ Mg km}^{-2} \text{ yr}^{-1}$) exceeds the productivity of 370–620 and 300–940 $\text{Mg km}^{-2} \text{ yr}^{-1}$ for warm-season and cool-season grasses in urban lawns (Springer, 2012). To the best of our knowledge there is no published information for warm species in urban turfs to compare these estimates.

The study in rural Singapore reported a biomass productivity of $876 \text{ Mg km}^{-2} \text{ yr}^{-1}$ for cowgrass (Ng et al., 2015). Cowgrass is frequently grown in oil palm, coconut and rubber plantations because of its high tolerance to shade, grazing and soil acidity, despite of being rated as a species of low forage productivity ($200\text{--}250 \text{ Mg km}^{-2} \text{ yr}^{-1}$). More productive grasses can produce up to $1400\text{--}1600 \text{ Mg km}^{-2} \text{ yr}^{-1}$ (Reynolds, 1995). Tropical grasslands under favorable conditions of high-water availability, warm temperature and continuing replenishment of nutrients can yield productivities of $1500\text{--}3000 \text{ Mg km}^{-2} \text{ yr}^{-1}$ (Woodwell and Whittaker, 1968).

Based on these figures, the biomass productivity in our residential lawn is lower than those of natural grasslands and pasture grasses under ideal conditions in the tropics, but higher than the productivity of urban lawns in temperate latitudes. Tropical humid evergreen forests, like those surrounding Singapore, have an average aboveground biomass accumulation of $1056 \pm 168 \text{ Mg km}^{-2} \text{ yr}^{-1}$ (Luyssaert et al., 2007); this is essentially the same biomass of harvested clippings in our lawn for one year. Consequently, management of clippings in urban lawns has large implications for the local carbon budget.

4.3. Net carbon flux budgets

Based on the carbon assimilated by photosynthesis and stored in soil and grass shoots, and the emissions related to fossil fuel consumption for maintenance activities (652 ± 1068 , 1671 ± 624 , and $27.0 \text{ Mg CO}_2 \text{ km}^{-2} \text{ yr}^{-1}$, respectively), under a steady state in which F_s relies only on the atmospheric CO_2 taken by photosynthesis (i.e., no contributions from organic material already in soil), the residential lawn assessed in this study can remove up to $2296 \pm 1692 \text{ Mg CO}_2 \text{ km}^{-2} \text{ yr}^{-1}$ ($626 \pm 461 \text{ Mg C km}^{-2} \text{ yr}^{-1}$) of atmospheric CO_2 . Depending on the gardening waste management (i.e., clippings disposal), this amount can decrease, and even shift the lawn to act as a net CO_2 source to the atmosphere. In the worst-case scenario, in which all harvested clippings were burnt, and the carbon stored by grass clippings returned to the atmosphere, the lawn would act as a net CO_2 source of $1046 \pm 1692 \text{ Mg CO}_2 \text{ km}^{-2} \text{ yr}^{-1}$ ($285 \pm 461 \text{ Mg C km}^{-2} \text{ yr}^{-1}$). Therefore, it is important that clippings can be used for compost or forage, or give them any other use that help to mitigate indirectly the emission of greenhouse gases.

The fate of the carbon produced belowground that does not return to the atmosphere through F_s was not investigated. The carbon content in soil was determined at the beginning of the study, but not at the end. Then, it was not possible to evaluate the buildup of a carbon pool throughout the study.

The consumption of CO_2 by mineral weathering reactions cannot be considered as a factor in the timescale assessed in this study (Trumbore, 2006); however, losses through leaching of dissolved carbon can





Mowing frequency				
	Trimmer	Push mower	Lawn tractor	Riding mower
Every week	78.2	82.6	70.1	28.0
Every 2 nd week	39.1	41.3	35.1	14.0
Every 3 rd week	25.6	27.0	22.9	9.2
Once per month	18.0	19.1	16.2	6.5

Fig. 7. Annual CO₂ emissions (Mg CO₂ km⁻² yr⁻¹) by fossil fuel consumption for turfgrass maintenance according to the mowing equipment and mowing frequency. See Table SM3 for detailed information on the equipment characteristics and emission factors for Singapore's conditions.

Table 2

Annual soil CO₂ efflux (F_s) rates for rural and urban grasslands reported in the literature for different climates and locations. For the case of natural and rural grasslands, as well as this study, values are geometric mean \pm one standard deviation computed from the available data. For the rest, values are mean \pm one standard deviation as reported by the authors. The F_s rates reported for Phoenix, USA, Seoul, Korea and Fort Collins, USA are for irrigated turfs, while those reported for Moscow, Russia and this study are for non-irrigated turfs.

Climate/Location	F_s (Mg CO ₂ km ⁻² yr ⁻¹)	Number of studies	Reference
Natural grasslands			
Tropical	869 \pm 524	3	Bond-Lamberty and Thomson (2018)
Subtropical and Mediterranean	1661 \pm 1624	27	Bond-Lamberty and Thomson (2018)
Temperate	2548 \pm 1881	253	Bond-Lamberty and Thomson (2018)
Unmanaged rural grasslands			
Tropical	4778 \pm 1111	6	Bond-Lamberty and Thomson (2018)
Subtropical and Mediterranean	3678 \pm 1445	14	Bond-Lamberty and Thomson (2018)
Temperate	2713 \pm 1932	48	Bond-Lamberty and Thomson (2018)
Managed rural grasslands			
Tropical Singapore	9852 \pm 347 ^a	1	Ng et al. (2015)
Subtropical and Mediterranean	2875 \pm 1819	214	Bond-Lamberty and Thomson (2018)
Temperate	2746 \pm 2346	122	Bond-Lamberty and Thomson (2018)
Urban turfgrasses			
Tropical Singapore	3370 \pm 812	–	This study
Subtropical Phoenix, USA	9386 \pm 880	–	Koerner and Klopatek (2002)
Temperate Seoul, Korea	3850 \pm 330	–	Bae and Ryu (2017)
Temperate Fort Collins, USA	10,182 \pm 1001	–	Kaye et al. (2005)
Temperate Moscow, Russia	13,182 \pm 352 ^b	–	Shchepeleva et al. (2017)

^a Based on periodic flux chamber measurements along a 5-month period.

^b Maximum annual rate among a set of non-irrigated experimental turfgrass plots.

happen. In temperate grasslands drainage fluxes exports roughly 25% of the atmospheric carbon removed by the ecosystem (Kindler et al., 2011). Belowground CO₂ may dissolve together with organic carbon in soil water, be transported convectively with percolating water, and reach the network of drains, canals and rivers that feed the city water reservoirs. Thus, leaching losses may become important because outgassing of carbon into the atmosphere from surface waters outside the boundaries of the studied lawn. In a similar way, the fraction of dissolved organic carbon may contribute to the eutrophication of water bodies. Grass clippings have been identified as a main source of nutrients in local ponds that contributes to frequent algal blooms (Wang and Joshi, 2013).

4.3.1. Turfgrass carbon contribution at neighborhood and national scale

If we consider that 15% of the neighborhood surface is covered by turfgrass (i.e., backyards, parks, verges) and assume that all green plots share the same characteristics of our experimental plot, then the carbon removed and stored by grass and soil across the neighborhood would be 344 Mg CO₂ km⁻² yr⁻¹. This budget represents 5.7% of the total CO₂ flux at the local scale, including contributions from all anthropogenic and natural sources and sinks, measured directly using a tall eddy covariance flux tower in the same neighborhood (Roth et al., 2017). However, this finding is only applicable under an ideal maintenance and waste disposal management, which effectively reduces the use of mowing equipment and avoids any CO₂ molecule already removed by vegetation to return to the atmosphere.

We highlight that if all clippings are collected and burnt, the beneficial service provided by turfgrass in this neighborhood would be lost. Instead, green plots would release 157 Mg CO₂ km⁻² yr⁻¹, which represents an increase of 2.6% to the total CO₂ emission.

We had previously estimated an annual carbon uptake of 165 Mg CO₂ km⁻² yr⁻¹ by all trees and palms planted in this neighborhood (3500 and 1900 trees km⁻², respectively) using allometric methods (Velasco et al., 2013; Velasco and Chen, 2019). Together with the carbon uptake by turfgrass, the entire biogenic component in this neighborhood might remove up to 510 Mg CO₂ km⁻² yr⁻¹ from the atmosphere, and offset 8% the local emissions of CO₂ under a disposal management in which none gardening waste ends burnt.

Fifteen percent of Singapore's land (112 km²) is classified as 'open green managed areas without trees' (i.e., turfgrass) (Gaw et al., 2019). According to our data, these areas could remove up to 257 or add 117 Gg CO₂ yr⁻¹, depending on the clippings' fate. These amounts represent an offset of 0.53% or an addition of 0.24% to the total CO₂ emissions from

energy consumption, industrial activities and waste incineration at city scale (48,567 Gg CO₂ yr⁻¹; NEA, 2018). Similarly, assuming that all turfgrass systems across the island city-state store a similar amount of carbon above and below ground, the carbon density of 2.24 kg C m⁻² estimated here indicates that Singapore's green carpet stores 919.9 Gg CO₂ (250.9 Gg C), a stock that represents 3.6 times its annual CO₂ flux, and 1.9% the annual emissions of anthropogenic origin.

The carbon stored by our lawn is in the lower range of those reported for lawns in temperate cities (Guertal, 2012 and reference therein), but similar to those reported for urban lawns and semi-rural grasslands covered by cowgrass in (sub)tropical locations. The carbon stock reported in this study is between those reported for Hong Kong's fertilized urban lawns (3.12 ± 0.44 kg C m⁻² accounting for aboveground biomass and 15-cm soil-depth; Kong et al., 2014) and that for the infrequently managed grassland of Singapore mentioned above (2.30 kg C m⁻² accounting for above and belowground biomass and topsoil; Ng et al., 2015).

4.4. Soil respiration responses and modeling challenges

Soil temperature, photosynthetic active radiation (PAR) and precipitation are apparently the main environmental factors that regulate F_s in tropical humid urban turfgrass systems. The supply of organic substrates is relatively constant and Θ_s variations are not significant to discourage microbial activity, thus T_s variations are expected to control heterotrophic respiration, while variations in PAR, autotrophic respiration. Unfortunately, our measurements cannot distinguish fluxes from each F_s component. Additional experiments as those described by Trumbore (2006) or modeling tests (e.g., Zhao et al., 2021) are needed to separate the autotrophic and heterotrophic contributions.

The mechanisms influenced by plant phenology and photosynthesis that control F_s are complex. Biological systems respond to present and past input stimuli, which regulate the timing and contribution of autotrophic and heterotrophic activity (Vargas et al., 2011b). For grasslands and short stature vegetation, it has been observed that F_s is in phase with variations in T_s and gross primary productivity because F_s responds fast to changes in photosynthesis, as freshly assimilated carbon is rapidly transferred belowground and utilized for F_s processes (Bahn et al., 2009; Vargas et al., 2011a). The availability of carbohydrates for autotrophic activity is apparently strongly regulated by PAR through photosynthesis (Mitra et al., 2019).

Our results show that F_s has a similar diurnal asymmetry to that observed for the total CO₂ flux measured at neighborhood scale by a flux tower (see Fig. 2 in Velasco et al., 2013). These results suggest that photosynthesis is an important CO₂ flux component in highly vegetated urban areas in the tropics. Under severe environmental conditions (i.e., high radiation, temperature and vapor pressure deficit), plants experience stomatal closure as a mechanism to prevent water loss through evapotranspiration, which reduces photosynthesis. Since autotrophic respiration is a direct consequence of root respiration, which is coupled to photosynthesis (Baldocchi et al., 2006), harsher weather conditions depressing turfgrass' photosynthesis may explain the lower F_s in the afternoon. Through isotope partitioning, Carbone et al. (2008) observed that the diurnal pattern of F_s in a semi-arid perennial grassland was largely controlled by autotrophic activity. Assuming constraints on photosynthesis due to physiological responses to water-stress, they modelled a hypothetical radiocarbon signature for root respiration that showed the same pattern and asymmetry than the F_s observed in our case.

The constant high Θ_s triggered by frequent rainfall prevents soil respiration pulse events and diminishes F_s during short periods. Additional moisture in an already wet soil ($\Theta_s > 0.15 \text{ m}^3 \text{ m}^{-3}$) reduces the soil diffusivity of CO₂ even more, as well as limits root and microbial metabolism by reducing oxygen availability for respiration (Vargas et al., 2010). This is contrary to water-limited ecosystems, where precipitation can trigger F_s spikes, especially after long dry spells, by

changing soil diffusivity, increasing photosynthates, and enhancing microbial activity and plant metabolism (Vargas et al., 2018). Future studies in tropical lawns should pay attention to drain after intense rains. Water-logging is an important factor for soil oxidation. Signs of redoximorphic features could help to evaluate the oxidation effects after water saturation (Vepraska et al., 2018). The non-stationary nature of these events and the diversity of underlying mechanisms complicate its modeling. Empirical models based on T_s and Θ_s responses usually fail to reproduce rapid F_s changes. In this study, the exponential correlation based on both parameters (eq. (4)) somewhat reproduces the rapid decline after intense rainfall (Fig. 5), but masks the biophysical processes that regulate F_s . The Q_{10} model is blind to those sudden declines, thus during periods affected by frequent downpours overpredicts F_s , but not during 'dry' periods as the dry spell of a few days shown in Fig. 5.

Our results show that empirical models are able to accurately predict F_s at monthly- and annual-scales, but these models are limited to predict the high-frequency (i.e., 30-min intervals) measurements. The overall CO₂ flux emitted from soil results from an integration of many physical and biological processes that do not necessarily fully correlate with T_s and Θ_s (especially in tropical ecosystems), and their responses may end confounded by factors that covary with them (e.g., photosynthesis rate, microbial activity, soil physical properties, plant phenology, nutrient and litter availability). However, these models can explain up to 90% of the seasonal and annual variation for the site where they were developed, as the integration of such processes loses relevance in the long-term (Trumbore, 2006). More complex models are needed to simulate F_s at high temporal resolution. For example, highly parametrized models using machine learning approaches are a promising approach to simulate the daily, and even hourly variability of F_s (Vargas et al., 2018).

5. Conclusions

Our results suggest that urban lawns in Singapore can act either as a sink or as an emission source of CO₂, depending on the clippings waste management. Year round warm and humid conditions enhance biomass productivity, as well as soil carbon production and storage. Soil CO₂ efflux (F_s) is relatively constant throughout the year, but this flux is not particularly high and does not exceed the amount of carbon assimilated by photosynthesis, which drives a net accumulation of carbon in biomass and soil. However, the fate of clippings ultimately determines the lawns' role as a net carbon sink or emission source. If grass clippings are incinerated, the lawn acts as a net emission source of CO₂ to the atmosphere.

The CO₂ fluxes reported here provide insight on the relevance of the components that regulate the carbon dynamics in turfgrass systems. The locally derived models to estimate F_s , CO₂ production (P_s) and storage (S_s), and aboveground biomass productivity of grass can be used to improve the accounting of carbon stocks and fluxes at a city scale bearing in mind some uncertainty due to variations in soil and grass characteristics, and management practices. An assessment of these variations across the city's green areas, together with the addition of sensors to monitor soil temperature and moisture to existing weather stations will improve the accuracy of such models.

Although the carbon removal or emission associated to turfgrass systems represents a minor fraction of the greenhouse gas budget at a city scale, it is important to identify and implement gardening practices that promote carbon storage and reduce the impact of maintenance activities. These practices must be tailored to local climate, topography, cultural and social conditions. Planting native species that adapt to the site and soil characteristics will eliminate the need for fertilization and irrigation, or soil quality improvement. Priority should be given to green areas covered by trees and not only by turfgrass to increase carbon sequestration. Lawns and parklands should be designed to reduce soil disturbance and maintenance activities. Mowing frequency should be based on turfgrass health rather than on aesthetic appearance. Mowing equipment should be chosen based on mowing performance and CO₂

emission rates. String trimmers should be avoided as much as possible, while leaf blowers should not be used at all. If clippings cannot be left in place to decay, a proper disposal management should be implemented. Greenery waste could be used for compost or to produce biofuel. Animal grazing could be an alternative to reduce mowing emissions and clippings waste generation. Finally, bold alternatives to decorative grounds such as lawns covered by native and spontaneous vegetation instead of monotonous grass might reduce the environmental impact of current greenery designs, while creating dense biodiverse and low-maintenance green plots that could be used by the public for recreational and educational purposes.

Credit author statement

Erik Velasco, Conceptualization, Methodology, Software, Validation, Formal analysis, Investigation, Resources, Data curation, Writing – original draft, Supervision, Project administration, Funding acquisition. Elvagrís Segovia, Methodology, Validation, Formal analysis, Investigation, Resources, Data curation, Writing – review & editing. Amy M. F. Choong, Investigation, Writing – review & editing. Benjamin K. Y. Lim, Investigation, Formal analysis, Data curation, Writing – review & editing. Rodrigo Vargas, Methodology, Software, Writing – review & editing.

Declaration of competing interest

The authors declare that they have no known competing financial interests or personal relationships that could have appeared to influence the work reported in this paper.

Acknowledgements

The field measurements were supported by the National Research Foundation Singapore through the Singapore MIT Alliance for Research and Technology's CENSAM laboratory. CENSAM stopped activities and closed its doors on Dec. 2017. A research fellowship granted to E. Velasco by the Centre for Urban Greenery and Ecology (CUGE) of Singapore's National Park Board (NParks) allowed to complete the data postprocessing and analysis, and prepare this publication. Conversations with CUGE's researchers, in particular with A. Yee, N. Goh, H. Ibrahim, S. Ghosh and S.K. Ling, were fundamental to learn on NParks' scientific needs for practical and regulatory purposes, and prepare the article in such context.

Appendix A. Supplementary data

Supplementary data to this article can be found online at <https://doi.org/10.1016/j.jenvman.2020.111752>.

References

- Bae, J., Ryu, Y., 2017. Spatial and temporal variations in soil respiration among different land cover types under wet and dry years in an urban park. *Landscape Urban Planning* 167, 378–385.
- Bahn, M., Schmitt, M., Siegwolf, R., Richter, A., Brüggemann, N., 2009. Does photosynthesis affect grassland soil-respired CO₂ and its carbon isotope composition on a diurnal timescale? *New Phytologist* 182 (2), 451–460.
- Baldocchi, D., Tang, J., Xu, 2006. How switches and lags in biophysical regulators affect spatial-temporal variation of soil respiration in an oak-grass savanna. *J. Geophys. Res.: Biogeosciences* 111.
- Bond-Lamberty, B.P., Thomson, A.M., 2018. A Global Database of Soil Respiration Data, Version 4.0. ORNL DAAC, Oak Ridge, Tennessee, USA (Available at:).
- Carbone, M.S., Winston, G.C., Trumbore, S.E., 2008. Soil respiration in perennial grass and shrub ecosystems: linking environmental controls with plant and microbial sources on seasonal and diel timescales. *J. Geophys. Res.: Biogeosciences* 113, G02022.
- Centre for Urban Greenery & Ecology CUGE, 2010. Guidelines for Tropical Turfgrass Installation and Management. CS B01:2010. National Parks Board, Singapore.
- Chapin, F.S., Woodwell, G.M., Randserson, J.T., Rastetter, E.B., Lovett, G.M., Baldocchi, D.D., Clark, D.A., Harmon, M.E., Schimel, D.S., Valentini, R., Wirth, C., 2006. Reconciling carbon-cycle concepts, terminology, and methods. *Ecosystems* 9 (7), 1041–1050.
- Cueva, A., Bullock, S.H., López-Reyes, E., Vargas, R., 2017. Potential bias of daily soil CO₂ efflux estimates due to sampling time. *Sci. Rep.* 7, 11925.
- Decina, S.M., Hutryra, L.R., Gately, C.K., Getson, J.M., Reinmann, A.B., Gianotti, A.G.S., Templer, P.H., 2016. Soil respiration contributes substantially to urban carbon fluxes in the greater Boston area. *Environ. Pollut.* 212, 433–439.
- Falk, J.H., 1976. Energetics of a suburban lawn ecosystem. *Ecology* 57 (1), 141–150.
- Falk, J.H., 1980. The primary productivity of lawns in a temperate environment. *J. Appl. Ecol.* 17, 689–696.
- Gaw, L.Y.F., Yee, A.T.K., Richards, D.R., 2019. A high-resolution map of Singapore's terrestrial ecosystems. *Data* 4 (116).
- Ghosh, S., Scharenbroch, B.C., Ow, L.F., 2016. Soil organic carbon distribution in roadside soils of Singapore. *Chemosphere* 165, 163–172.
- Guertal, E.A., 2012. Carbon sequestration in turfed landscapes: a review. In: Rattan, L., Augustin, B. (Eds.), *Carbon Sequestration in Urban Ecosystems*. Springer, Dordrecht, pp. 197–213.
- Hiller, R.V., McFadden, J.P., Kljun, N., 2011. Interpreting CO₂ fluxes over a suburban lawn: the influence of traffic emissions. *Boundary-Layer Meteorol.* 138 (2), 215–230.
- Jo, H.K., McPherson, G.E., 1995. Carbon storage and flux in urban residential greenspace. *J. Environ. Manag.* 45, 109–133.
- Johnson, T., 2018. Best weed-eater shootout – string trimmers gas powered. OPEREVIEW.com. Available at: <https://opereviews.com/buying-guides/best-weed-eater-shootout-gas-powered/>.
- Kaye, J.P., McCulley, R.L., Burke, I.C., 2005. Carbon fluxes, nitrogen cycling, and soil microbial communities in adjacent urban, native and agricultural ecosystems. *Global Change Biol.* 11, 575–587.
- Kim, D.G., Vargas, R., Bond-Lamberty, B., Turetsky, M.R., 2012. Effects of soil rewetting and thawing on soil gas fluxes: a review of current literature and suggestions for future research. *Biogeosciences* 9 (7), 2459–2483.
- Kindler, R., Siemens, J.A.N., Kaiser, K., Walmsley, D.C., Bernhofer, C., Buchmann, N., Cellier, P., Eugster, W., Gleixner, G., Grünwald, T., Heim, A., et al., 2011. Dissolved carbon leaching from soil is a crucial component of the net ecosystem carbon balance. *Global Change Biol.* 17, 1167–1185.
- Koerner, B., Klopatek, J., 2002. Anthropogenic and natural CO₂ emission sources in an arid urban environment. *Environ. Pollut.* 116, S45–S51.
- Kong, L., Shi, Z., Chu, L.M., 2014. Carbon emission and sequestration of urban turfgrass systems in Hong Kong. *Sci. Total Environ.* 473, 132–138.
- Leitgeb, E., Ghosh, S., Dobbs, M., Englisch, M., Michel, K., 2019. Distribution of nutrients and trace elements in forest soils of Singapore. *Chemosphere* 222, 62–70.
- Lerman, S.B., Contosta, A.R., 2019. Lawn mowing frequency and its effects on biogenic and anthropogenic carbon dioxide emissions. *Landscape Urban Planning* 182, 114–123.
- Livesley, S.J., Dougherty, B.J., Smith, A.J., Navaud, D., Wylie, L.J., Arndt, S.K., 2010. Soil-atmosphere exchange of carbon dioxide, methane and nitrous oxide in urban garden systems: impact of irrigation, fertiliser and mulch. *Urban Ecosyst.* 13 (3), 273–293.
- Luyssaert, S., Inghima, I., Jung, M., Richardson, A.D., Reichstein, M., Papale, D., Piao, S.L., Schulze, E.D., Wingate, L., Matteucci, G., Aragos, L., Aubinet, M., Beer, C., Bernhofer, C., Black, K.G., Bonal, D., Bonnefond, M., Chambers, J., Ciais, P., Cook, B., Davis, K.J., Dolman, A.J., Gielen, B., Goulden, M., Grace, J., Granier, A., Grelle, A., Griffis, T., Grünwald, T., Guidolotti, G., Hanson, P.J., Harding, R., Hollinger, D.Y., Hutryra, L.R., Kolari, P., Kruijt, B., Kutsch, W., Lagergren, F., Laurila, T., Law, B.E., Le Maire, G., Lindroth, A., Loustau, D., Malhi, Y., Matus, J., Migliavacca, M., Misson, L., Montagnani, L., Moncrieff, J., Moors, E., Munger, J.W., Nikinmaa, E., Ollinger, S.V., Pita, G., Rebmann, C., Roupsard, O., Saigusa, N., Sanz, M.J., Seufert, G., Sierra, C., Smith, M.L., Tang, J., Valentini, R., Vesala, T., Janssens, I.A., 2007. CO₂ balance of boreal, temperate, and tropical forests derived from a global database. *Global Change Biol.* 13, 2509–2537.
- Mahecha, M.D., Reichstein, M., Carvalhais, N., Lasslop, G., Lange, H., Seneviratne, S.I., Vargas, R., Ammann, C., Arain, M.A., Cescatti, A., Janssens, I.A., 2010. Global convergence in the temperature sensitivity of respiration at ecosystem level. *Science* 329, 838–840.
- Maier, M., Schack-Kirchner, H., 2014. Using the gradient method to determine soil gas flux: a review. *Agric. For. Meteorol.* 192, 78–95.
- Mandapaka, P.V., Qin, X., 2013. Analysis and characterization of probability distribution and small-scale spatial variability of rainfall in Singapore using a dense gauge network. *Journal of Applied Meteorology and Climatology* 52 (12), 2781–2796.
- Mitra, B., Miao, G., Minick, K., McNulty, S.G., Sun, G., Gavazzi, M., King, J.S., Noormets, A., 2019. Disentangling the effects of temperature, moisture, and substrate availability on soil CO₂ efflux. *J. Geophys. Res.: Biogeosciences* 124 (7), 2060–2075.
- Moldrup, P., Olesen Yamaguchi, T., Schjonning, P., Rolston, D.E., 1999. Modeling diffusion and reaction in soils: IX. The Buckingham-Burdine-Campbell equation for gas diffusivity in undisturbed soil. *Soil Sci. Soc. Am.* 63, 542–551.
- Monteiro, J.A., 2017. Ecosystem services from turfgrass landscapes. *Urban For. Urban Green.* 26, 151–157.
- National Environmental Agency NEA, 2018. Singapore's Fourth National Communication and Third Biennial Update Report under the United Nations Framework Convention on Climate Change. National Environmental Agency (NEA), Singapore.
- Ng, B.J.L., Hutryra, L.R., Nguyen, H., Cobb, A.R., Kai, F.M., Harvey, C., Gandois, L., 2015. Carbon fluxes from an urban tropical grassland. *Environ. Pollut.* 203, 227–234.
- Nowak, D.J., Greenfield, E.J., Hoehn, R.E., Lapoint, E., 2013. Carbon storage and sequestration by trees in urban and community areas of the United States. *Environ. Pollut.* 178, 229–236.

- Or, D., Wraith, 2002. Soil water content and water potential relationships. In: Warrick, A. W. (Ed.), *Soil Physics Companion*. CRC Press LLC, Boca Raton, FL, USA, pp. 49–84.
- Pahari, R., Leclerc, M.Y., Zhang, G., Nahravi, H., Raymer, P., 2018. Carbon dynamics of a warm season turfgrass using the eddy-covariance technique. *Agric. Ecosyst. Environ.* 251, 11–25.
- Pataki, D.E., Carreiro, M.M., Cherrier, J., Grulke, N.E., Jennings, V., Pincetl, S., Pouyat, R.V., Whitlow, T.H., Zipperer, W.C., 2011. Coupling biogeochemical cycles in urban environments: ecosystem services, green solutions, and misconceptions. *Front. Ecol. Environ.* 9 (1), 27–36.
- Reynolds, S.G., 1995. Pasture-cattle-coconut systems. *Food and agriculture organization of the united Nations*. Available at: <http://www.fao.org/3/af298e/af298E00.htm#TOC>.
- Roth, M., Jansson, C., Velasco, E., 2017. Multi-year energy balance and carbon dioxide fluxes over a residential neighbourhood in a tropical city. *Int. J. Climatol.* 37, 2679–2698.
- Saxton, K.E., Rawls, W.J., 2006. Soil water characteristic estimates by texture and organic matter for hydrologic solutions. *Soil Sci. Soc. Am. J.* 70, 1569–1578.
- Shechepeleva, A.S., Vasenev, V.I., Mazirov, I.M., Vasenev, I.I., Prokhorov, I.S., Gosse, D. D., 2017. Changes of soil organic carbon stocks and CO₂ emissions at the early stages of urban turf grasses' development. *Urban Ecosyst.* 20 (2), 309–321.
- Springer, T.L., 2012. Biomass yield from an urban landscape. *Biomass Bioenergy* 37, 82–87.
- Tang, J., Baldocchi, D.D., Qi, Y., Xu, L., 2003. Assessing soil CO₂ efflux using continuous measurements of CO₂ profiles in soils with small solid-state sensors. *Agric. For. Meteorol.* 118, 207–220.
- Tang, J., Misson, L., Gershenson, A., Cheng, W., Goldstein, A.H., 2005. Continuous measurements of soil respiration with and without roots in a ponderosa pine plantation in the Sierra Nevada Mountains. *Agric. For. Meteorol.* 132, 212–227.
- Townsend-Small, A., Czimczik, C.I., 2010. Carbon sequestration and greenhouse gas emissions in urban turf. *Geophys. Res. Lett.* 37, L02707.
- Trumbore, S., 2006. Carbon respired by terrestrial ecosystems—recent progress and challenges. *Global Change Biol.* 12, 141–153.
- United Nations, 2018. *The World's Cities in 2018—Data Booklet*. Department of Economic and Social Affairs, Population Division. New York, NY, USA, ISBN 978-92-1-047610-2.
- USA-EPA, 2018. MOVES2014, MOVES2014a, and MOVES2014b Technical Guidance. EPA-420-B-10-039. August 2018. Available at: <https://www.epa.gov/moves/latest-version-motor-vehicle-emission-simulator-moves>.
- Vargas, R., Allen, M.F., 2008. Diel patterns of soil respiration in a tropical forest after Hurricane Wilma. *J. Geophys. Res.: Biogeosciences* 113, G03021.
- Vargas, R., Baldocchi, D.D., Allen, M.F., Bahn, M., Black, T.A., Collins, S.L., Yuste, J.C., Hirano, T., Jassal, R.S., Pumpanen, J., Tang, J., 2010. Looking deeper into the soil: biophysical controls and seasonal lags of soil CO₂ production and efflux. *Ecol. Appl.* 20 (6), 1569–1582.
- Vargas, R., Baldocchi, D.D., Bahn, M., Hanson, P.J., Hosman, K.P., Kulmala, L., Pumpanen, J., Yang, B., 2011a. On the multi-temporal correlation between photosynthesis and soil CO₂ efflux: reconciling lags and observations. *New Phytol.* 191 (4), 1006–1017.
- Vargas, R., Carbone, M.S., Reichstein, M., Baldocchi, D.D., 2011b. Frontiers and challenges in soil respiration research: from measurements to model-data integration. *Biogeochemistry* 102, 1–13.
- Vargas, R., Sánchez-Cañete, E., Serrano-Ortiz, P., Yuste, J.V., Domingo, F., López-Ballesteros, A., Oyonarte, C., 2018. Hot-moments of soil CO₂ efflux in a water-limited grassland. *Soil Systems* 2 (3), 47.
- Velasco, E., Chen, K.W., 2019. Carbon storage estimation of tropical urban trees by an improved allometric model for aboveground biomass based on terrestrial laser scanning. *Urban For. Urban Green.* 44, 126387.
- Velasco, E., Roth, M., Tan, S.H., Quak, M., Nabarro, S.D.A., Norford, L., 2013. The role of vegetation in the CO₂ flux from a tropical urban neighbourhood. *Atmos. Chem. Phys.* 13, 10185–10202.
- Vepraska, M.J., Lindbo, D.L., Stolt, M.H., 2018. Redoximorphic features. In: Stoops, G., Marelino, V. (Eds.), *Interpretation of Micromorphological Features of Soils and Regoliths*, second ed. Mees. Elsevier B.V., pp. 425–445.
- Vogt, C.A., Kho, C., Sia, A., 2017. Urban greening and its role in fostering human well-being. In: Tan, P.Y., Jim, C.Y. (Eds.), *Greening Cities: Forms and Functions*. Springer Nature, Singapore, pp. 95–111.
- Waller, S.S., Lewis, J.K., 1979. Occurrence of C₃ and C₄ photosynthetic pathways in North American grasses. *J. Range Manag.* 32 (1), 12–28.
- Wang, J., Joshi, U.M., 2013. *Improving Water Quality in Tropical Urban Ponds: a Case Study in East Coast Park*. Research Technical Note. Urban Ecology Series RTN08-2013. Singapore's National Parks Board. Available at: <https://www.nparks.gov.sg/cuge>.
- Warner, D.L., Bond-Lamberty, B., Jian, J., Stell, E., Vargas, R., 2019. Spatial predictions and associated uncertainty of annual soil respiration at the global scale. *Global Biogeochem. Cycles* 33 (12), 1733–1745.
- Weissert, L.F., Salmond, J.A., Schwendenmann, L., 2014. A review of the current progress in quantifying the potential of urban forests to mitigate urban CO₂ emissions. *Urban Climate* 8, 100–125.
- Weissert, L.F., Salmond, J.A., Schwendenmann, L., 2016. Variability of soil organic carbon stocks and soil CO₂ efflux across urban land use and soil cover types. *Geoderma* 271, 80–90.
- Woodwell, G.M., Whittaker, R.H., 1968. Primary production in terrestrial ecosystems. *Am. Zool.* 8, 19–30.
- Yee, A.T.K., Chong, K.Y., Seah, W.W., Lua, H.K., Yang, S., 2019. *Vegetation of Singapore*. Flora of Singapore 1, 47–70.
- Zhao, X., Liang, N., Zeng, J., Mohti, A., 2021. A simple model for partitioning forest soil respiration based on root allometry. *Soil Biol. Biochem.* 152, 108067.
- Zirkle, G., Lal, R., Augustin, B., 2011. Modeling carbon sequestration in home lawns. *Hortscience* 46 (5), 808–814.